A LAGRANGIAN MEAN VIEW OF EVENTS IN A BOUNDED TURBULENT FLOW

W.R.C Phillips
Department of Mathematics, School of Science
Swinburne University of Technology
Hawthorn Victoria 3122, Australia
wrphilli@illinois.edu

ABSTRACT

This paper is concerned with Lagrangian mean counterparts of familiar Reynolds stresses which arise in turbulent shear flows. The measures are the drift, akin to the Reynolds shear stress and the pseudomomentum, a measure of the turbulence intensity. Phillips (2001) has succinctly expressed the measures in terms of Lagrangian integrals of Eulerian space-time correlations. However they are difficult to interpret and so the present work begins by expressing them in a more insightful form. Both measures are calculated for turbulent channel flow for a range of Reynolds numbers up to $\mathrm{Re}_\tau = 5200$. The pseudomomentum is always negative and has a sole peak located in wall units in the low teens while at the highest Reynolds number studied, the drift is negative in the vicinity of that peak, positive elsewhere and largest near the rigid boundary. Finally, the drift and pseudomomentum are discussed in the context of coherent wall layer structures with which they are intricately linked.

INTRODUCTION

Kraichnan (1977, 1976) long ago showed that a Lagrangian representation of fluid motion has the advantage of capturing more physics than an Eulerian one. His Lagrangian perturbation theory, however, presumes a specific representation of Lagrangian motion and restricts attention to a generalized velocity field $\mathbf{u}(\mathbf{x},t|s)$, defined as the velocity measured at time s in a fluid element which passes through $\mathbf{x}$ at time t. On the other hand, if the traditional Lagrangian representation is employed and an exact mapping of Navier Stokes then taken into a Lagrangian mean reference frame, we arrive at the generalized Lagrangian mean (GLM) equations (Andrews & McIntyre, 1978), which can be written in a form not unlike those given by a simple Reynolds average but with the familiar Reynolds stresses replaced by the unfamiliar drift and the pseudomomentums (Phillips, 1998*a*). To be precise, GLM parses fluid motion into unambiguous mean and oscillatory parts, thereby yielding precise definitions for the drift, which expresses the mean mass transport in excess (or deficit) of any Eulerian mean flow, and the pseudomomentum, which determines the force exerted by the fluctuating motion on the medium (Phillips, 2015).

Drift and pseudomomentum are Lagrangian averages of interacting velocity fluctuations and thus arise in many circumstances in the physical sciences, an example being Stokes (1847) drift. But while Stokes drift occurs in irrotational monochromatic surface waves in quiescent surroundings, the drift in a sheared turbulent flow results from a fluctuating field that is rotational and interacts with the shear. Because of that the mathematics describing it is significantly more complicated.

Consider, for example, the Lagrangian velocity u_i^ξ (with components $i = 1,2,3$) of a particle initially at position $\mathbf{x}$ that follows a path determined by the displacement $\boldsymbol{\xi}(\mathbf{x},t)$ in terms of an Eulerian velocity field $u_i(\mathbf{x},t)$. Then

$$u_i^\xi(\mathbf{x},t) = u_i(\mathbf{x}+\boldsymbol{\xi}(\mathbf{x},t),t) \tag{1}$$

and for fluctuations of slope $\epsilon \ll 1$ and $\boldsymbol{\xi} = O(\epsilon)$, a Taylor series expansion yields:

$$u_i^\xi(\mathbf{x},t) = u_i + \xi_j u_{i,j} + \frac{1}{2}\xi_j\xi_k u_{i,jk} + \ldots \tag{2}$$

The Lagrangian mean velocity $\overline{u}_i^\xi$ is obtained by averaging (2) over the time scale of the fluctuations and noting that u_i may comprise both mean $\overline{u}_i$ and fluctuating $\breve{u}_i$ parts, as $u_i = \overline{u}_i + \breve{u}_i$. So, since the drift d_i is the difference between $\overline{u}_i^\xi$ and the Eulerian mean $\overline{u}_i$, then (Phillips, 1998*a*)

$$d_i = \overline{u}_i^\xi - \overline{u}_i = \overline{\xi_j\breve{u}_{i,j}} + \frac{1}{2}\overline{\xi_j\xi_k}\overline{u}_{i,jk} + \ldots, \tag{3}$$

which reduces to the Stokes drift when $\overline{u}_i = 0$. Accordingly the pseudomomentum is

$$p_i = -\overline{\xi_{j,i}u_j^\ell}, \tag{4}$$

where $u_j^\ell = \breve{u}_j + \xi_k\overline{u}_{j,k}$ (Andrews & McIntyre, 1978).

Observe that in contrast with their Eulerian-mean Reynolds stress counterparts, which are second-order correlations of velocity, the drift and pseudomomentum are second-order correlations of velocity and displacement. These can, of course, be evaluated in closed form for simple oscillatory flows (Stokes, 1847; Phillips *et al.*, 2010), but that is not the case for fluctuating fields comprised of a spectrum of wavenumbers. Rather, with a spectrum it is

expeditious to re-express the velocity-displacement correlations in terms of velocity correlations. That said doing so is not straightforward, but it can be achieved (Phillips, 2001); we then find that (3) and (4) are expressed in terms of Lagrangian integrals of Eulerian space-time correlations, as (5) and (6).

Unfortunately even with the integral form to hand the space-time correlations therein are difficult to acquire and the few available from experiments and numerics are not broad enough to evaluate (5) and (6). To proceed, therefore, Phillips (2000) developed a model for two point two-time velocity correlations and used it with DNS results to calculate the drift and pseudomomentum in turbulent channel flow for $\mathrm{Re}_\tau = 180$ (Phillips, 2001). He found that the drift is oriented in the flow direction (that is positive) only near the wall with a zero at around thirteen wall units, while the pseudomomentum peaks near the zero in drift and is never positive. Of immediate interest, of course, is whether these findings carry over to higher Reynolds numbers (Phillips, 2015) and we shall explore that herein using Lee & Moser's (2015) DNS data to $\mathrm{Re}_\tau = 5200$.

That said, our motivation for evaluating the measures is broader than Reynolds number dependence and indeed rests with how best to characterize the structure of turbulent flows and whether a Lagrangian mean approach will reveal more about the structure than an Eulerian one. To that end we note the relationship between drift and coherent structures, namely robust, reoccurring concentrations of vorticity that form near boundaries in turbulent shear flows and live over timescales long with respect to the fluctuating motions.

The structures are characterized by velocity perturbations in the streamwise direction, known as streaks, and cross-stream perturbations that realize streamwise aligned rolls; streaks and rolls together comprise a vortex. The association of the drift with these vortices is twofold: first, the vorticity (vortex lines) from which they form moves at the Lagrangian mean velocity, given by the sum of the Eulerian mean velocity and the drift (3). Accordingly, Lagrangian mean field theory indicates that the redistribution of vorticity necessary to the formation of the vortices is effected by differential drift (and or pseudomomentum) and mean shear (Phillips, 1998*a*).

Known too is that such structures are self-sustaining, in the sense that streaks spawn streamwise aligned rolls, which in turn spawn streaks, through what some researchers (Hall & Smith, 1988; Bennett *et al.*, 1991; Hall & Sherwin, 2010) describe as a Rayleigh vortex-wave interaction and others (Jimnez & Moin, 1991; Keefe *et al.*, 1992; Waleffe, 1995; Hamilton *et al.*, 1995) describe as regeneration. Numerical studies further show that "plane wave modes are present (and) play an important if not essential role in turbulent wall bounded flows" (Sirovich *et al.*, 1990). Nevertheless, in spite of the ubiquity of vortices and waves being well established and the genesis of the waves well understood, the genesis of the vortices remains unclear.

To that end we take two paths: first, since much is known about the mechanics of the vortices in terms of Reynolds stress and shear (Sreenivasan & Sahay, 1997; Klewicki *et al.*, 2007), we want to clarify the role of these properties in the drift and pseudomomentum. Second, we want to utilize the drift and pseudomomentum in Lagrangian mean field theory to explore the origin of the vortices (Phillips, 1998*a*, 2015).

FORMULATION

In order to deduce the measures (3) and (4), Phillips (2001) considers a fluctuating finite amplitude three-dimensional disturbance defined by a spectrum of wavenumbers riding on a parallel Eulerian mean shear flow $U(z)$ of constant density aligned in the x direction with y cross stream and z normal to the wall. He shows that the streamwise component of the drift $D_1(z)$, which has dimensions of velocity, is:

$$D_1 = -\frac{\partial}{\partial z}\int_0^{\tau^\star} Q_{31}\,d\tau - \frac{1}{2}\frac{d^2U}{dz^2}\int_{\tau^\star}^0\int_0^\zeta Q_{33}\,d\tau d\zeta, \quad (5)$$

while the streamwise component of pseudomomentum, which likewise has dimensions of velocity, is

$$\begin{aligned} P_1 = &\int_0^{\tau^\star}\frac{\partial}{\partial r}Q_{jj}\,d\tau + \frac{dU}{dz}\int_{\tau^\star}^0\int_0^\zeta \frac{\partial}{\partial r}(Q_{31}-Q_{13})\,d\tau d\zeta \\ &+ \left(\frac{dU}{dz}\right)^2\int_{\tau^\star}^0\int_0^\chi\int_{\tau^\star}^\zeta \frac{\partial}{\partial r}Q_{33}\,d\tau d\zeta d\chi. \end{aligned} \quad (6)$$

Herein Q_{ij} are space-time correlations at time delay τ and spatial delay $r = U\tau$, while ζ and χ are dummy variables for τ. Moreover $\tau^*(z)$ is a unique value of τ determined by integral constraints (Phillips, 2001, 2015).

Unfortunately Q_{ij} is not easily acquired. Because of that Phillips (2000) modeled it using the Kovasznay-Corrsin (Kovasznay, 1953; Corrsin, 1959) conjecture, which in essence says that Q_{ij} is separable as magnitude, set by the one point velocity correlation $\overline{\breve{u}_i\breve{u}_j}$, hereafter written as $\overline{u_iu_j}$, and the unity normalized correlation R_{ij}, rendering

$$Q_{ij}(z;\mathbf{r},\tau) = \overline{u_iu_j}(z)\,R_{ij}(U\tau,0,0,\tau). \quad (7)$$

To evaluate (7) we thus require U, $\overline{u_iu_j}$ and R_{ij}. Details of U and $\overline{u_iu_j}$ are available for specific Reynolds numbers from direct simulations and any Reynolds number from asymptotically correct integral expressions for boundary layer and channel flows (Phillips, 1987; Phillips & Ratnanather, 1990; Phillips, 1994). The correlation R_{ij} is given in Phillips (2000).

Drift and Pseudomomentum

On substituting (7) into (5), (6) and introducing the Lagrangian velocity scales $\mathscr{A}$, $\mathscr{B}$, $\mathscr{C}$, $\mathscr{U}$, $\mathscr{V}$ and $\mathscr{W}$ defined in terms of R_{ij} in (10)-(11), we find approximations for the drift (Phillips, 2015)

$$-D_1 = \frac{d}{dz}\left(\mathscr{A}\,\overline{uw}\right) + \mathscr{B}^2\,\overline{w^2}\,\frac{d^2U}{dz^2} \quad (8)$$

and pseudomomentum

$$-P_1 = \frac{\overline{u^2}}{\mathscr{U}} + \frac{\overline{v^2}}{\mathscr{V}} + \frac{\overline{w^2}}{\mathscr{W}}\left[1 + \left(\mathscr{C}\frac{dU}{dz}\right)^2\right]. \quad (9)$$

We see that the drift is closely related to differential Reynolds stress $\overline{uw}$ while the pseudomomentum is related

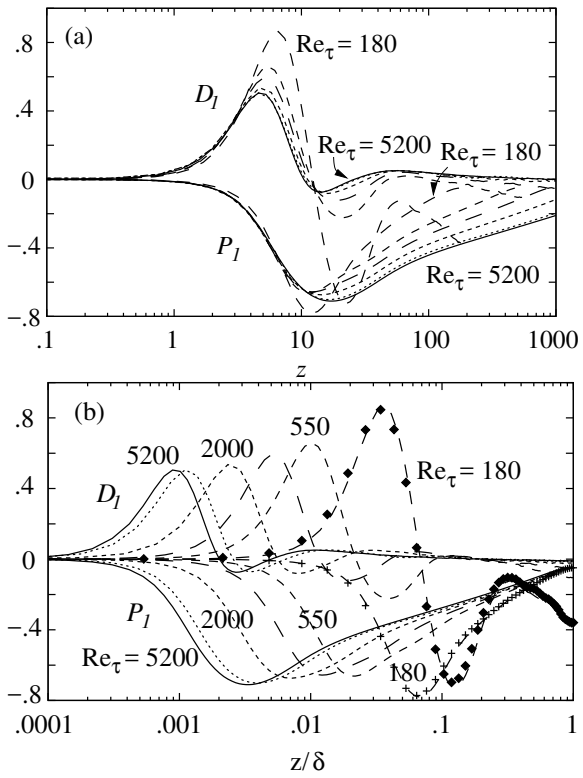

Figure 1. Profiles of drift D_1 and pseudomomentum P_1 normalized by U_τ for turbulent channel flow as a function of distance from the wall in: (a) wall units and (b) outer units. Herein Re_τ = 180, 550, 1000, 2000, 4200 and 5200; D_1 ◆ and P_1 + at Re_τ = 180 from Phillips (2001).

to the turbulence intensities $\overline{u^2}$, $\overline{v^2}$ and $\overline{w^2}$. Herein the Lagrangian time scales are:

$$\mathscr{A} = \int_0^{\tau^\star} R_{31} d\tau, \quad \mathscr{B}^2 = -\frac{1}{2}\int_{\tau^\star}^0 \int_0^\zeta R_{33} d\tau d\zeta \qquad (10)$$

and

$$\mathscr{C}^2 = -\mathscr{W} \int_{\tau^\star}^0 \int_0^\chi \int_{\tau^\star}^\zeta \frac{\partial}{\partial r} R_{33} d\tau d\zeta d\chi, \qquad (11)$$

while the velocity scales are

$$[\mathscr{U}^{-1}, \mathscr{V}^{-1}, \mathscr{W}^{-1}] = -\int_0^{\tau^\star} \frac{\partial R_{jj}}{\partial r} d\tau. \qquad (12)$$

RESULTS

The drift (8) and pseudomomentum (9) were calculated using the DNS data of Lee & Moser (2015) at Re_τ = 180, 550, 1000, 2000 and 5200, with data by Lozano-Duran & Jiménez (2014) at Re_τ = 4200. Unless otherwise specified results are given in wall units, which defer to length $\nu/\tilde{U}_\tau$ and time $\nu/\tilde{U}_\tau^2$ scales, linked by the friction velocity $\tilde{U}_\tau = (\nu d\tilde{U}/d\tilde{z}|_{\mathrm{wall}})^{\frac{1}{2}}$, with $Re_\tau = \delta = \tilde{\delta}\tilde{U}_\tau/\nu$.

Reynolds number dependence

To deduce the dependence of drift and pseudomomentum on Reynolds number the results are plotted at all Re_τ in both wall units (figure 1(a)) and outer units (figure 1(b)), where the independent variable is z/δ.

Looking first at the drift with increasing distance from the wall in wall units, we observe collapse, or close to it, for all Re_τ only in the viscous sublayer. Each profile then goes on to a peak that is positive and diminishes with increased Re_τ. Profiles for all Re_τ then intersect at much the same location $z = z_f \in (13, 14)$. Furthermore, since the drift is negative at z_f all profiles necessarily exhibit a zero at $z < z_f$. A second peak, this one negative, occurs in the buffer layer near $z \in (15, 25)$; this peak diminishes in magnitude and moves towards z_f as Re_τ increases. Near $z \in (30, 60)$, as the buffer layer is transitioning to the logarithmic region, the profiles reach a third peak. This peak is positive for all cases except Re_τ = 180 and from it the drift varies monotonically to its centerline value, a value that is markedly negative at the lowest Re_τ but essentially zero at the highest Re_τ. Finally, while all profiles exhibit consistent behavior across the channel domain, they appear to relax, as Re_τ increases, to the profile at the highest Re_τ. Indeed there is little difference between the curves at the two highest Re_τ, with the inference that the drift is asymptotic to a limiting form and that the Re_τ = 5200 results are close to that form.

On the other hand the pseudomomentum is much simpler than the drift and is always negative. Looking in more detail we find as z increases that, in contrast to the drift, collapse extends into the buffer layer, to approximately $z = 10$. The profiles peak in the vicinity of but not at z_f and then relax, irrespective of Re_τ, to approximately the same nonzero centerline value.

When viewed in outer units (figure 1(b)), on the other hand, the profiles for both measures are distinctly separate not only in the inner region as we would expect, but also in the outer region where our mindset is some degree of collapse. Of course each profile depicts a clear logarithmic decay and may be asymptotic to a distinct curve in the outer region.

Time and velocity scales

The mean velocity, variance and covariance collapse in the wall region, so the lack of collapse depicted by D_1 and P_1 in figure 1(a) in the wall region must, in view of (8) and (9), reflect a Reynolds number dependence in the time ($\mathscr{A}, \mathscr{B}, \mathscr{C}$) and velocity scales ($\mathscr{U}, \mathscr{V}, \mathscr{W}$).

The time scales are plotted in figures 2(a) and 2(b), the former at Re_τ = 180 and the latter at Re_τ = 5200. Observe that the value of each scale at $z = 0$ and $z/\delta = 1$ is little affected by Re_τ. Moreover, all profiles are essentially constant in the sublayer and ultimately (in fact over much of the layer) grow with distance from the wall. But the profiles in the interior and specifically in the wall region, are affected by Reynolds number. This dependence is particularly evident in the differential of $\mathscr{A}$, as we observe in figure 3 although, in line with our earlier findings, it diminishes with increasing Reynolds number, suggesting that $\mathscr{A}$, $\mathscr{B}$ and $\mathscr{C}$ approach a terminal form.

Lastly we plot, in figures 4(a) and 4(b), the velocity scales at the lowest and highest Re_τ. Here we find that although the scales have the same generic form, to wit initially constant and ultimately almost logarithmic, the details are very much Reynolds number related. For example the low Reynolds number results for $\mathscr{U}$ and $\mathscr{V}$ exhibit two re-

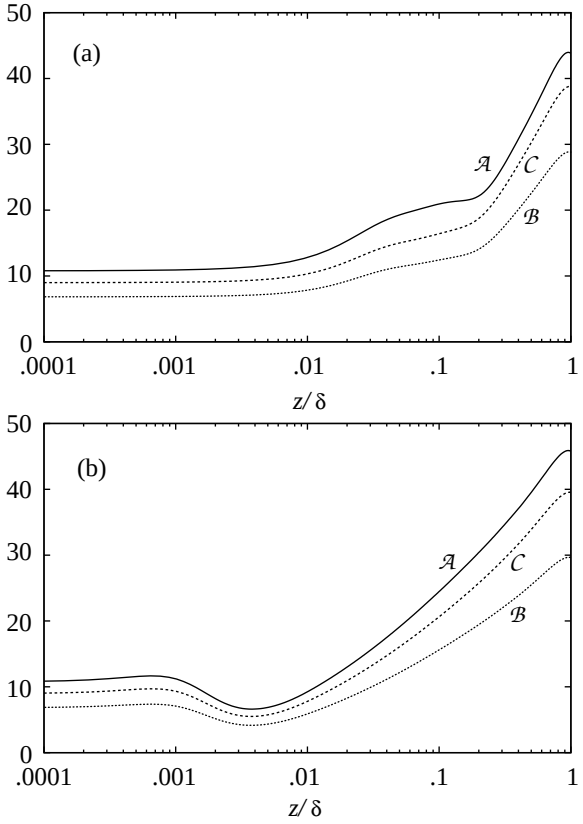

Figure 2. Profiles of the time scales $\mathscr{A}$, $\mathscr{B}$, $\mathscr{C}$ in wall units as a function of distance z from the boundary in outer units, for channel flow at (a) $\mathrm{Re}_\tau = 180$ and (b) $\mathrm{Re}_\tau = 5200$.

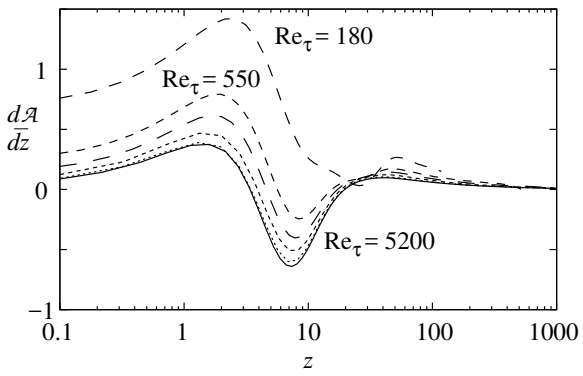

Figure 3. Differential time scale $d\mathscr{A}/dz$ as a function of distance z from the boundary in wall units, for channel flow at $\mathrm{Re}_\tau = 180$, 550, 1000, 2000, 4200 and 5200.

gions of growth, while the higher ones do not. Also, in contrast to the time scales, the end values at $z = 0$ and $z/\delta = 1$ change significantly with Reynolds number, although much of that dependence is offset when the scales are utilized in (9) and all is summated to depict P_1.

Coherent structures

How though do the drift and pseudomomentum affect or effect the etiology of wall layer structures? Looking first to the drift, we saw that its sign is mixed throughout the layer; specifically that it is positive in the viscous sublayer, negative for much of the buffer region and, depending on the Reynolds number, mixed in the logarithmic and outer

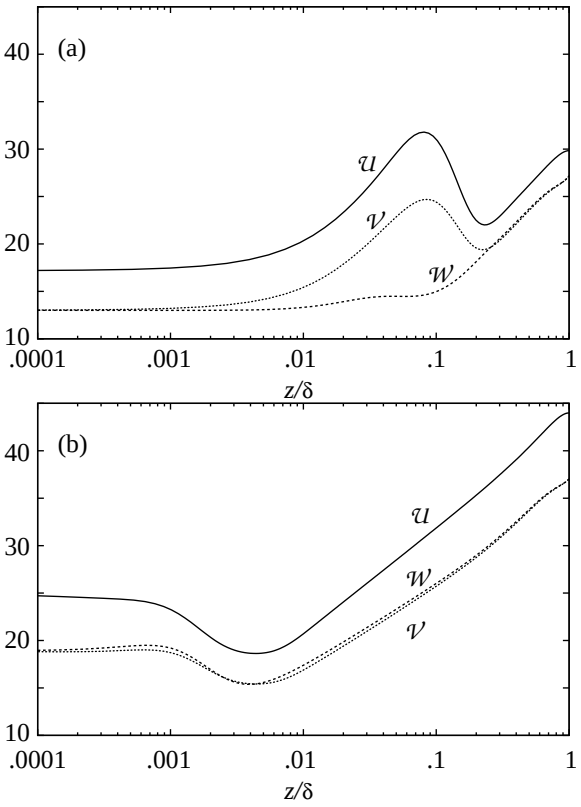

Figure 4. Profiles of the velocity scales $\mathscr{U}$, $\mathscr{V}$, $\mathscr{W}$ in wall units as a function of distance z from the boundary in outer units for channel flow at (a) $\mathrm{Re}_\tau = 180$ and (b) $\mathrm{Re}_\tau = 5200$.

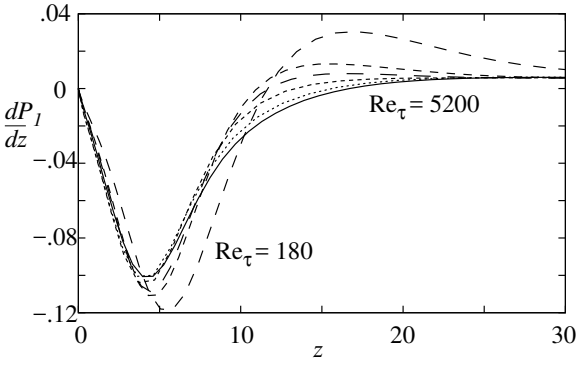

Figure 5. Differential pseudomomentum dP_1/dz with distance z from the boundary in wall units, for $\mathrm{Re}_\tau = 180$, 550, 1000, 2000, 4200 and 5200.

regions. These alternating layers of positive and negative drift are clearly evident in figure 1(a) along with the finding that it appears to approach a terminal form as Reynolds number increases. At all Reynolds numbers, however, the drift is strongest immediately adjacent to the wall and is dominated in that region by the term $d\mathscr{A}\overline{uw}/dz$. Indeed, because $\overline{uw}$ plays such a key role, it is instructive to rewrite (8) in a manner that highlights $\overline{uw}$, *viz*

$$-D_1 = \frac{d\overline{uw}}{dz}\left(\mathscr{A} + \mathscr{B}^2\,\overline{w^2}\right) + \overline{uw}\,\frac{d\mathscr{A}}{dz} - \frac{\mathscr{B}^2\,\overline{w^2}}{\delta}. \qquad (13)$$

Of course the prominence of $\overline{uw}$ in the drift should come as no surprise, because the importance of of $\overline{uw}$ to the me-

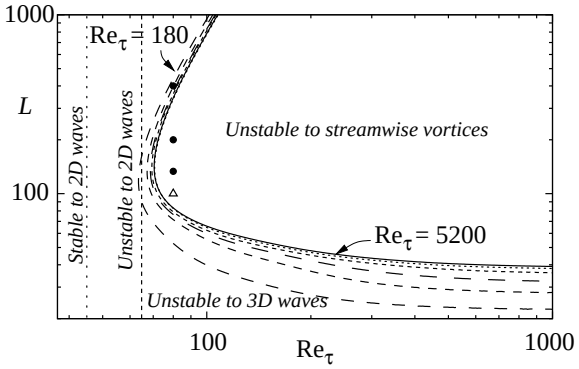

Figure 6. Stability boundaries for the onset of streamwise vortex structure depicted by the linear steady states of CLg theory (Phillips, 1998*a*) describing periodic Poiseuille flow for Re_τ = 180, 550, 1000, 2000, 4200 and 5200, expressed as streak spacing L (2 rolls) in wall units against Re_τ. The asymptotes for instability to two- and three-dimensional waves determined numerically are drawn at $\mathrm{Re}_\tau = 45$ and $\mathrm{Re}_\tau = 64.8$ (Orszag & Patera, 1983). Numerical results for • Roll spacing and △ ensemble average of streak spacing at $\mathrm{Re}_\tau = 80$ (Sirovich *et al.*, 1990).

chanics of bounded turbulent shear flow and the presence of near wall structure has long been known, as has the importance is its wall normal derivative and where that derivative is zero (Sreenivasan & Sahay, 1997).

Specifically, we know that its derivative is zero in the log region where, from Townsend's (1976) attached eddy hypothesis, asymptotic analysis (Phillips, 1987; Phillips & Ratnanather, 1990) and numerous high Reynolds number experiments (Marusic *et al.*, 2013)

$$\overline{u_i^2} = A_i - B_i \ln\left(\frac{z}{\delta}\right) \quad \text{for} \quad (i = 1, 2, 3). \tag{14}$$

Here $B_3 = 0$ and the remaining A_i and B_i are positive constants, so $\overline{w^2} \sim A_3$. Moreover, because $\overline{uw} \sim -1$ in the log region, (13) then reduces to

$$D_1 \sim \frac{d\mathscr{A}}{dz} + \frac{\mathscr{B}^2 A_3}{\delta}. \tag{15}$$

Furthermore, we find from figures 2 and 3 that the second term in (15) dominates in the log region, which means that the drift varies as $\mathscr{B}^2$, that is logarithmically with z, as does the pseudomomentum and mean velocity.

We thus associate the large scale roll-mode structures observed in the log region with this logarithmic variation in drift and the more intense near wall structures with drift dominated by $d\overline{uw}/dz$, which necessarily varies algebraically (Phillips, 1987). Of course each can be identified with an exact coherent state solution (Nagata, 1990; Waleffe, 1998), one adjacent to the wall and the other further out (Deguchi & Hall, 2014). But the inner and outer structures would appear to be not closely coupled, because rough walls are known to obliterate only those near wall, not those further out.

But what of the origin of the vortices? On a vastly different scale stadium sized vortices form in the upper ocean through the interaction of differential drift and shear (Craik & Leibovich, 1976). We emphasize that the instability mechanism exciting them is *not* the same as would occur in a bounded turbulent flow, nevertheless the generalized theory describing the later does retain the seminal idea of the former, *vis-à-vis* the interaction of differential drift and/or pseudomomentum and shear.

The generalized theory is built on the premise that the time scales of the shear and coherent structures are long with respect to the time scales of the fluctuating field and, along with drift and pseudomomentum, is also derived from GLM. Several instabilities to streamwise vortices are possible under this theory but the one of relevance is the CLg instability (Craik, 1982; Phillips, 1998*a*, 2003). Herein the velocity scale of the streaks far exceeds that of the rolls, which results in the streaks acting to modulate the fluctuating field. Interestingly, although modulation initially suppresses the instability (Phillips & Wu, 1994), it ultimately acts as a catalyst to a self sustaining streak-roll process (Phillips, 1998*b*) not unlike those proposed by Hall & Smith (1988) and Waleffe (1995). The question remaining, of course, is whether the structure depicted by CLg theory using our distributions of drift and pseudomomentum concur with observations of wall layer structure and we conclude by addressing that question.

Key to CLg instability theory is differential pseudomomentum and we see in figure 5 that the differential is largely negative and confined to the sublayer and buffer layer regions, so streamwise vortices would occur there provided the Craik-Phillips-Shen criterion (Craik, 1982; Phillips, 2003) to instability to streamwise vortices is satisfied, which it is (Phillips & Shen, 1996). In view of that Phillips (2015) explores instability further. He does so by first assuming that integral features of the turbulent flow field are captured by periodic Poiseuille flow, that is pressure driven flow between parallel horizontal plates subjected to waves traveling in the flow direction. The flow is doubly periodic (streamwise and spanwise) and as Reynolds number increases the interaction is unstable first to two and subsequently three dimensional waves (Orszag & Kells, 1980) whose amplitudes grow until inhibited by nonlinearities, at which point the flow equilibrates (Rozhdestvensky & Simakin, 1984; Keefe *et al.*, 1992). Key here is that equilibrated flow comprised of 24 modes "reflect(s) the basic integral properties of turbulent flows rather well" (Rozhdestvensky & Simakin, 1984). In fact only 16 modes are necessary to ensure U depicts logarithmic behavior (Keefe *et al.*, 1992). Phillips (2015) solves for the steady states that determine the stability boundary to the formation of streamwise vortices.

As plotted in figure 6, the boundary depicts the streak spacing L determined by a counter-rotating vortex pair, against Re_τ. Included therein are asymptotes for instability to two- and three-dimensional waves, *viz* $\mathrm{Re}_\tau = 45$ and $\mathrm{Re}_\tau = 64.8$ (Orszag & Patera, 1983), the later of which is closely consistent with our $\mathrm{Re}_\tau = 63.5$ onset boundary to streamwise vortices and the theoretical minimum value ($\mathrm{Re}_\tau \approx 68.7$) at which U can exhibit logarithmic behavior (Phillips, 1994). Consistent too are spacings found numerically at $\mathrm{Re}_\tau = 80$ (Sirovich *et al.*, 1990). Finally, we note that onset, depicted by the nose of the curves, occurs at $L \approx 120$ wall units, a value near the widely observed circa 100 mean streak spacing first reported by Kline *et al.* (1967). Thus, to conclude, Lagrangian mean field theory not only captures key structural features in the wall region but also isolates a key (not sole) instability mechanism responsible for their formation, namely CLg.

ACKNOWLEDGEMENT

My thanks to Joseph Klewicki and Philip Hall for insightful discussions. This work was supported by grants from the National Science Foundation OCE-0116921 and the Australian Research Council DP1093517.

REFERENCES

Andrews, D. G. & McIntyre, M. E. 1978 An exact theory of nonlinear waves on a Lagrangian-mean flow. *J. Fluid Mech.* **89**, 609–646.

Bennett, J., Hall, P. & Smith, F. T. 1991 The strong nonlinear interaction of Tollmien-Schlichting waves and Taylor-Görtler vortices in curved channel flow. *J. Fluid Mech.* **223**, 475–495.

Corrsin, S. 1959 Lagrangian correlation and some difficulties in turbulent diffusion experiments. In *Atmospheric diffusion and air pollution* (ed. F. N. Frenkiel & P. A. Sheppard), pp. 441–446. Academic, New York.

Craik, A. D. D. 1982 Wave induced longitudinal-vortex instability in shear flows. *J. Fluid Mech.* **125**, 37–52.

Craik, A. D. D. & Leibovich, S. 1976 A rational model for Langmuir circulations. *J. Fluid Mech.* **73**, 401–426.

Deguchi, K. & Hall, P. 2014 Free-stream coherent structures in parallel boundary-layer flows. *J. Fluid Mech.* **752**, 602–625.

Hall, Philip & Sherwin, Spencer 2010 Streamwise vortices in shear flows: harbingers of transition and the skeleton of coherent structures. *J. Fluid Mech.* **661**, 178–205.

Hall, P. & Smith, F.T. 1988 The nonlinear interaction of Görtler vortices and Tollmien-Schlichting waves in curved channel flows. *Proc. R. Soc. Lond. A* **417**, 255–282.

Hamilton, James M., Kim, John & Waleffe, Fabian 1995 Regeneration mechanisms of near-wall turbulence structures. *J. Fluid Mech.* **287**, 317–348.

Jimnez, Javier & Moin, Parviz 1991 The minimal flow unit in near-wall turbulence. *J. Fluid Mech.* **225**, 213–240.

Keefe, L., Moin, P. & Kim, J. 1992 The dimension of attractors underlying periodic turbulent Poiseuille flow. *J. Fluid Mech.* **242**, 1–29.

Klewicki, J C, Fife, P, Wei, T & McMurtry, P 2007 A physical model of the turbulent boundary layer consonant with mean momentum balance structure. *Phil. Trans. R. Soc. A* **365** (1852), 823–840.

Kline, S. J., Reynolds, W. C., Schraub, F. A. & Runstadler, P. W. 1967 The structure of turbulent boundary layers. *J. Fluid Mech.* **30**, 741–773.

Kovasznay, L. S. G. 1953 Turbulence in supersonic flow. *J. Aero. Sci.* **20**, 657–674.

Kraichnan, Robert H. 1976 Diffusion of passive-scalar and magnetic fields by helical turbulence. *J. Fluid Mech.* **77**, 753–768.

Kraichnan, Robert H. 1977 Lagrangian velocity covariance in helical turbulence. *J. Fluid Mech.* **81**, 385–398.

Lee, M. & Moser, R. D. 2015 Direct numerical simulation of turbulent channel flow up to $Re_\tau = 5200$. *J. Fluid Mech.* **774**, 395–415.

Lozano-Duran, A. & Jiménez, J. 2014 Effect of the computational domain on direct simulations of turbulent channels up to Re_τ=4200. *Phys. Fluids* **26**, 011702.

Marusic, I., Monty, J. P., Hultmark, M. & Smits, A. J. 2013 On the logarithmic region in wall turbulence. *J. Fluid Mech.* **716**, R3.

Nagata, M. 1990 Three-dimensional finite-amplitude solutions in plane Couette flow: bifurcation from infinity. *J. Fluid Mech.* **217**, 519–527.

Orszag, S. A. & Kells, L. C. 1980 Transition to turbulence in plane Poiseuille and plane Couette flow. *J. Fluid Mech.* **96**, 159–205.

Orszag, S. A. & Patera, A. T. 1983 Secondary instability of wall-bounded shear flows. *J. Fluid Mech.* **128**, 347–385.

Phillips, W. R. C. 1987 The wall region of a turbulent boundary layer. *Phys. Fluids* **30** (8), 2354–2361.

Phillips, W. R. C. 1994 On the logarithmic-law constants and the turbulent boundary layer at low Reynolds numbers. *Appl. Sci. Res.* **52** (4), 279–293.

Phillips, W. R. C. 1998*a* Finite-amplitude rotational waves in viscous shear flows. *Stud. Appl. Math.* **101** (1), 23–47.

Phillips, W. R. C. 1998*b* On the nonlinear instability of strong wavy shear to longitudinal vortices. In *Nonlinear Instability, Chaos and Turbulence* (ed. L. Debnath & D. N. Riahi), pp. 277–299. Singapore: WIT Press.

Phillips, W. R. C. 2000 Eulerian space–time correlations in turbulent shear flows. *Phys. Fluids* **12** (8), 2056–2064.

Phillips, W. R. C. 2001 On the pseudomomentum and generalized Stokes drift in a spectrum of rotational waves. *J. Fluid Mech.* **430**, 209–229.

Phillips, W. R. C. 2003 Langmuir circulations. In *Wind-Over-Waves II: Forecasting and Fundamentals of Applications* (ed. S.G. Sajjadi & J.C.R. Hunt), pp. 157–167. Horwood Pub.

Phillips, W. R. C. 2015 Drift and pseudomomentum in bounded turbulent shear flows. *Phys. Rev. E* **92**, 043003.

Phillips, W. R. C., Dai, A. & Tjan, K. K. 2010 On Lagrangian drift in shallow-water waves on moderate shear. *J. Fluid Mech.* **660**, 221–239.

Phillips, W. R. C. & Ratnanather, J. T. 1990 The outer region of a turbulent boundary layer. *Phys. Fluids* **2** (3), 427–434.

Phillips, W. R. C. & Shen, Q. 1996 A family of wave-mean shear interactions and their instability to longitudinal vortex form. *Stud. Appl. Math.* **96** (2), 143–161.

Phillips, W. R. C. & Wu, Z. 1994 On the instability of wave-catalysed longitudinal vortices in strong shear. *J. Fluid Mech.* **272**, 235–254.

Rozhdestvensky, B. L. & Simakin, I. N. 1984 Secondary flows in a plane channel: their relationship and comparison with turbulent flows. *J. Fluid Mech.* **147**, 261–289.

Sirovich, L., Ball, K. S. & Keefe, L. R. 1990 Plane waves and structures in turbulent channel flow. *Phys. Fluids A* **2** (12), 2217–2226.

Sreenivasan, K. R. & Sahay, A. 1997 The persistence of viscous effects in the overlap region, and the mean velocity in turbulent pipe and channel flows. In *Self-Sustaining Mechanisms of Wall Turbulence* (ed. R. Panton), pp. 253–272. Computational Mechanics Publications, Southampton, UK.

Stokes, G. G. 1847 On the theory of oscillatory waves. *Trans. Camb. Phil. Soc.* **8**, 441–455.

Townsend, A.A. 1976 *The Structure of Turbulent Shear Flow*, 2nd edn. Cambridge University Press.

Waleffe, Fabian 1995 Hydrodynamic stability and turbulence: beyond transients to a self-sustaining process. *Stud. Appl. Math.* **95** (3), 319–343.

Waleffe, Fabian 1998 Three-dimensional coherent states in plane shear flows. *Phys. Rev. Lett.* **81**, 4140–4143.